

Multivariate data assimilation of GRACE, SMOS, SMAP measurements for improved regional soil moisture and groundwater storage estimates

Tangdamrongsub, Natthachet; Han, Shin Chan; Yeo, In Young; Dong, Jianzhi; Steele-Dunne, Susan C.; Willgoose, Garry; Walker, Jeffrey P.

DOI

[10.1016/j.advwatres.2019.103477](https://doi.org/10.1016/j.advwatres.2019.103477)

Publication date

2020

Document Version

Final published version

Published in

Advances in Water Resources

Citation (APA)

Tangdamrongsub, N., Han, S. C., Yeo, I. Y., Dong, J., Steele-Dunne, S. C., Willgoose, G., & Walker, J. P. (2020). Multivariate data assimilation of GRACE, SMOS, SMAP measurements for improved regional soil moisture and groundwater storage estimates. *Advances in Water Resources*, 135, Article 103477. <https://doi.org/10.1016/j.advwatres.2019.103477>

Important note

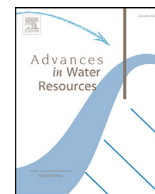
To cite this publication, please use the final published version (if applicable). Please check the document version above.

Copyright

Other than for strictly personal use, it is not permitted to download, forward or distribute the text or part of it, without the consent of the author(s) and/or copyright holder(s), unless the work is under an open content license such as Creative Commons.

Takedown policy

Please contact us and provide details if you believe this document breaches copyrights. We will remove access to the work immediately and investigate your claim.



Multivariate data assimilation of GRACE, SMOS, SMAP measurements for improved regional soil moisture and groundwater storage estimates

Natthachet Tangdamrongsub^{a,b,*}, Shin-Chan Han^c, In-Young Yeo^c, Jianzhi Dong^d, Susan C. Steele-Dunne^e, Garry Willgoose^c, Jeffrey P. Walker^f

^a Earth System Science Interdisciplinary Center, University of Maryland, College Park, MD, USA

^b Hydrological Sciences Laboratory, NASA Goddard Space Flight Center, Greenbelt, MD, USA

^c School of Engineering, Faculty of Engineering and Built Environment, The University of Newcastle, Callaghan, New South Wales, Australia

^d USDA-ARS Hydrology and Remote Sensing Lab, MD, USA

^e Department of Water Resources, Faculty of Civil Engineering and Geosciences, Delft University of Technology, Delft, the Netherlands

^f Department of Civil Engineering, Monash University, Clayton, Victoria, Australia

ARTICLE INFO

Keywords:

SMOS
SMAP
GRACE
EnKS
CABLE
Multivariate data assimilation
Soil moisture
Groundwater

ABSTRACT

Assimilating remote sensing observations into land surface models has become common practice to improve the accuracy of terrestrial water storage (TWS) estimates such as soil moisture and groundwater, for understanding the land surface interaction with the climate system, as well as assessing regional and global water resources. Such remote sensing observations include soil moisture information from the L-band Soil Moisture and Ocean Salinity (SMOS) and Soil Moisture Active Passive (SMAP) missions, and TWS information from the Gravity Recovery And Climate Experiment (GRACE). This study evaluates the benefit of assimilating them into the Community Atmosphere and Biosphere Land Exchange (CABLE) land surface model. The evaluation is conducted in the Goulburn River catchment, South-East Australia, where various in situ soil moisture and groundwater level data are available for validating data assimilation (DA) approaches. It is found that the performance of DA mainly depends on the type of observations that are assimilated. The SMOS/SMAP-only assimilation (SM DA) improves the top soil moisture but degrades the groundwater storage estimates, whereas the GRACE-only assimilation (GRACE DA) improves only the groundwater component. Assimilating both observations (multivariate DA) results in increased accuracy of both soil moisture and groundwater storage estimates. These findings demonstrate the added value of multivariate DA for simultaneously improving different model states, thus leading to a more robust DA system.

1. Introduction

Accurate knowledge on terrestrial water storage (TWS) is crucial for the assessment of climate variation and water resource availability (Entekhabi et al., 1996; Pitman, 2003; Rodell et al., 2007). The accuracy of TWS components (e.g., soil moisture, groundwater, snow, surface water) simulated by land surface models (LSM) at high spatial resolution is commonly degraded by uncertainties in meteorological forcing, model parameter calibration, and land surface process representation (Moradkhani et al., 2005; Wood et al., 2011). Hydrologic information can also be obtained from satellite remote sensing observations (e.g., Kerr et al., 2012; Maurer et al., 2003; Tapley et al., 2004). However, TWS components such as subsurface soil moisture and groundwater are usually not observed directly by in-situ observations, and the limited satellite coverage and sensing depths often restrict the reliability of the

observations (Reichle et al., 2008). Data assimilation (DA) can be used to combine various types of observations at different temporal and spatial resolutions with the model simulations according to the relative size of their errors (Reichle, 2008; Reichle et al., 2008). DA has been successfully applied in enhancing model-estimated hydrologic components such as TWS (e.g., Li et al., 2012), soil moisture (e.g., Lievens et al., 2015), groundwater (e.g., Tangdamrongsub et al., 2018b), snow (e.g., Andreadis and Lettenmaier, 2006), and runoff (e.g., Weerts and El Serafy, 2006).

Various satellite observations can be considered in the DA system to improve the key components of the TWS estimate. For example, surface soil moisture has an important role in the variability of the hydrological cycle and climate system (Entekhabi et al., 1996; Koster et al., 2009; Schumann et al., 2009) and can be measured by L-band radiometers, i.e., from the Soil Moisture and Ocean Salinity (SMOS; Kerr et al., 2012) and

* Corresponding author at: Hydrological Sciences Laboratory, NASA Goddard Space Flight Center, Greenbelt, MD, USA.
E-mail address: natthachet.tangdamrongsub@nasa.gov (N. Tangdamrongsub).

Soil Moisture Active Passive (Entekhabi et al., 2010) satellite missions (Chan et al., 2016). Both satellite missions provide global soil moisture products at a spatial resolution of $\sim 25 - 36$ km (representing the wetness in the top 0 – 5 cm soil layer) approximately every 3 days. The SMOS and SMAP radiometer data have been exploited in soil moisture data assimilation (SM DA) systems over several river basins, e.g., Ahlergaard (Western Denmark; Ridler et al., 2014), Murray-Darling (Lievens et al., 2015), continental Australia (e.g., Tian et al., 2017), the Great Lakes (Xu et al., 2015), and North America (e.g., Blankenship et al., 2016). These studies have demonstrated the benefits of SM DA on both surface and root zone soil moisture components (e.g., De Lannoy and Reichle, 2016; Tian et al., 2017; Xu et al., 2015). However, SM DA has been found to have a negative impact on the groundwater storage estimate (Tian et al., 2017).

In addition to the surface soil moisture, TWS variations (Δ TWS) can be derived from gravity measurements by the Gravity Recovery And Climate Experiment (GRACE) satellite mission (Tapley et al., 2004). The GRACE twin satellites measure changes of the Earth's gravity field every month using a combination of several measurements, including K-band ranging, accelerometer, attitude, and orbital data (Bettadpur, 2012). Because hydrological mass variations are dominant at a monthly time scale, the GRACE data are commonly presented in terms of Δ TWS, and have been used in a wide range of hydrological applications including data assimilation (e.g., Zaitchik et al., 2008; Eicker et al., 2014) for drought detection (e.g., Houborg et al., 2012; Li et al., 2012; Kumar et al., 2016), flood analysis (Reager et al., 2015), groundwater loss analysis (Giroto et al., 2017; Tangdamrongsub et al., 2018b), and snow estimation (Forman et al., 2012; Su et al., 2010). The benefit of GRACE DA was observed particularly in deep storage components such as groundwater storage (e.g., Tangdamrongsub et al., 2015; Zaitchik et al., 2008). However, GRACE DA is generally less effective in surface soil moisture improvement (Li et al., 2012; Tangdamrongsub et al., 2017a; Tian et al., 2017).

The goal of multivariate DA is to combine the strengths of SM DA and GRACE DA to simultaneously improve soil moisture and groundwater estimates. Tian et al. (2017) elaborated this concept and showed that the accuracy of surface and deep storage components could be improved by the application of GRACE and SMOS data assimilation. Similarly, Kumar et al. (2018) and Jasinski et al. (2019) applied multivariate DA using multiple satellite soil moisture and snow products to improve the skills of model state estimates and climate assessment indicators. Kumar et al. (2018) showed that the performance of DA is improved with new satellite sensors. Based on these findings, multivariate assimilation of GRACE and L-band satellite soil moisture sensors (e.g., SMOS, SMAP) is expected to lead to increased accuracy of soil moisture and groundwater estimates.

This study develops a multivariate DA with GRACE, SMOS, and SMAP data to improve the accuracy of regional soil moisture and groundwater storage estimates. The main research objective is to investigate the performance of multivariate DA in simultaneously improving soil moisture and groundwater storage estimates. Different DA schemes are developed to incorporate different observations into the DA system simultaneously. Three different DA scenarios subject to three different observation cases (SM-only, GRACE-only, and both) are evaluated in terms of estimating water storage (e.g., surface and root zone soil moisture, and groundwater). The DA approach is developed based on ensemble Kalman smoother (EnKS, see, e.g., Dunne et al., 2007; Dong et al., 2015; Tian et al., 2017; Tangdamrongsub et al., 2018b). The LSM used in this study is the Community Atmosphere and Biosphere Land Exchange (CABLE; Decker, 2015). The analysis is conducted over the Goulburn River catchment (Rüdiger et al., 2007) located in the eastern part of New South Wales, Australia, where extensive records of in situ soil moisture and groundwater are available from more than 20 sites throughout the catchment. The DA results are assessed by comparing them against the in situ data, and the ensemble open-loop estimate (EnOL, model run without DA). The evaluation is performed between January 2010 and

December 2015, when GRACE, SMOS, SMAP (from March 2015), and in situ data are available.

2. Materials

2.1. Study area

The Goulburn River catchment is located in the south-eastern part of the Murray-Darling basin and has a sub-humid or temperate climate (Fig. 1). The catchment has a total area of 6540 km² and consists of more than ten sub-catchments, including the Krui and Merriwa catchments where in situ soil moisture data are regularly recorded. The catchment is maintained by the Scaling and Assimilation of Soil Moisture and Streamflow (SASMAS) project (Rüdiger et al., 2007; <http://www.eng.newcastle.edu.au/sasmas/SASMAS/sasdata.html>). The land cover of the catchment consists of a floodplain, clear grassland, crop in the northern part, and a mountain range with dense vegetation in the south. The northern part of the catchment is particularly suitable for satellite soil moisture remote sensing studies due to its low to moderate vegetation cover. Furthermore, the clay content of the top soil layer (0 – 5 cm) in the northern part is several times greater than in the south (Senanayake et al., 2019; <http://www.clw.csiro.au/aclep/soilandlandscapegrid>). Higher variability in the top soil moisture can, therefore, be anticipated in the northern area. The mean annual rainfall of the catchment is ~ 700 mm and reaches ~ 1100 mm in the higher altitude areas. Monthly mean minimum/maximum temperatures reach approximately 16°/30 °C in summer and 2°/14°C in winter. No snowfall is presented in the catchment. LSM simulations are expected to perform well over the catchment due to the absence of groundwater abstraction and streamflow control.

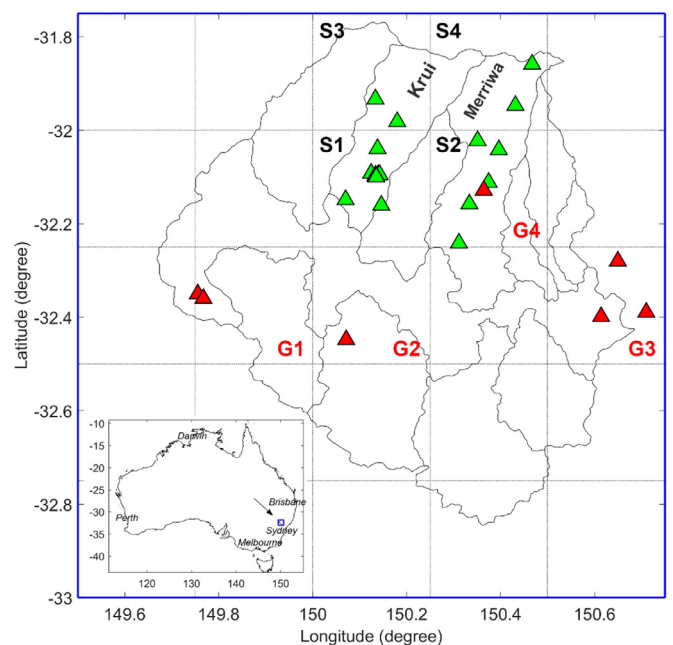


Fig. 1. The geographical location of the Goulburn River catchment, located in South-East Australia (see the inserted map). The black dotted squares indicate the 25 km model grid cells while the blue boundary denotes the GRACE grid cell used in this study. The locations of the in situ soil moisture and groundwater data are shown as green and red triangles, respectively. All in situ soil moisture data inside the same model grid cell are averaged, resulting in S1 – S4 in situ soil moisture grid cells. A similar approach is applied to the in situ groundwater data, resulting in G1 – G4 in situ groundwater grid cells. (For interpretation of the references to color in this figure legend, the reader is referred to the web version of this article.)

2.2. Land surface model setup

The Community Atmosphere and Biosphere Land Exchange (CABLE) land surface model is used to simulate daily volumetric soil moisture and groundwater storage at approximately 25 km resolution (see Fig. 1). The model can be obtained from <https://trac.nci.org.au/trac/cable>, and the model user guide and descriptions can be found in Decker (2015), Kowalczyk et al. (2006), and Ukkola et al. (2016). CABLE estimates soil moisture in six separate layers. In this study, the soil thicknesses from the top to bottom compartments are set to 1.2, 3.8, 25, 39.9, 107.9, 287.2 cm, respectively. In comparison with the in situ data (see Section 2.5), the combination of the first two model soil layers represents the 0 – 5 cm soil moisture component while the combination of the first three denotes the 0 – 30 cm component. The forcing data used in CABLE are precipitation, air temperature, snowfall rate, wind speed, humidity, surface pressure, and shortwave and longwave downward radiation. Similar to Tangdamrongsub et al. (2018a), the model is forced with meteorological input from the Global Land Data Assimilation System (GLDAS; Rodell et al., 2004). Following the sensitivity study of Tangdamrongsub et al. (2018a), GLDAS precipitation is replaced by data from the Tropical Rainfall Measuring Mission (TRMM; Huffman et al., 2007) to improve the performance of the CABLE model.

Two primary error sources of the LSM are the meteorological forcing data and the model parameters. In the DA process (see Section 3), the precipitation is perturbed based on the uncertainty provided by the TRMM product (Huffman, 1997). The shortwave radiation is perturbed using multiplicative white noise, with 10% of the nominal values. An additive white noise is used for the air temperature. It is acknowledged that while a homoscedastic error would be more realistic for air temperature, an offline sensitivity analysis found that the temperature error had only a marginal influence on the state estimates compared to e.g. precipitation. The errors of forcing data are assumed to be spatially correlated. As such, an exponential correlation function is applied to the covariance matrix for each forcing variable. The correlation lengths for forcing data were determined using variogram analysis and found to be approximately 25 km. Model parameters associated with soil moisture and groundwater components are also perturbed with a magnitude of 10%. The selected model parameters are the fractions of clay/sand/silt and the drainage parameters that control the soil storage capacity and amount of subsurface runoff, respectively. Both have a direct impact on the soil moisture and groundwater storages (see Table 2 in Tangdamrongsub et al. (2018a) for more details). The perturbation sizes of forcing data and parameters are determined based on the ensemble verification measures (De Lannoy et al., 2006), mainly to allow an adequate spread of the ensemble between updates in the DA process. Table 1 summarizes the forcing and parameter perturbation of this study. Note that the model state is not perturbed directly, but rather perturbed as a result of model propagation associated with the perturbed forcing and perturbed model parameters. As a result, the correlation between soil layers is mainly controlled by LSM physics, and

there is no artificially additional imposed error correlation between soil layers.

2.3. GRACE data processing

The GRACE data release 05 (RL05), provided by the Center for Space Research (CSR), the University of Texas Austin (Bettadpur, 2012), is obtained between January 2010 and December 2015. The product consists of the monthly spherical harmonic coefficient (SHC) complete up to degree and order 96. The full error variance-covariance matrix is also provided as a part of the product. The error matrix is only available up to June 2014, and the monthly average values are used for the missing months (July 2014 – Dec 2015). The GRACE-derived Δ TWS and its uncertainty over the Goulburn catchment are computed following the approach in Tangdamrongsub et al. (2017b). First, the degree 1 coefficients (SHC) provided by Swenson et al. (2008) are restored, and the C20 term is replaced by the value estimated from the satellite laser ranging (Cheng and Tapley, 2004). Second, the long-term mean (January 2010 – December 2015) is computed and removed from the monthly product to obtain the SHC variations, and the destriping (Swenson and Wahr, 2006) and 300-km radius Gaussian smoothing filters (Jekeli, 1981) are applied to the SHC variations to suppress the high-frequency noise. Third, the TWS variation (Δ TWS) is computed from the filtered SHC variations using the method described by Wahr et al. (1998). Because the GRACE-derived Δ TWS shows no significant spatial variability over the study area, the catchment averaged Δ TWS is used in this study. Finally, a signal restoration (e.g., Chen et al., 2014) is applied to the computed Δ TWS to restore the damped signal caused by the applied filters. The method iteratively searches for the genuine Δ TWS using a forward model constructed solely from the GRACE data. To be consistent with the model estimate, the temporal mean value of TWS (January 2010 – December 2015) from the CABLE estimate is added to the GRACE-derived Δ TWS to obtain the absolute TWS prior to the assimilation process. Finally, the TWS uncertainty is computed based on the GRACE full error-variance covariance matrix using error propagation (see, e.g., Tangdamrongsub et al. (2017b)). As GRACE error is spatially correlated in nature (Swenson and Wahr, 2006), deriving the error from the available full covariance matrix represents a more realistic GRACE uncertainty compared to the application of a uniform error value (e.g., Tangdamrongsub et al., 2015).

2.4. Satellite soil moisture observations

The daily satellite soil moisture retrievals derived from the Soil Moisture and Ocean Salinity (SMOS, Kerr et al., 2012) and the Soil Moisture Active Passive (SMAP, Entekhabi et al., 2010) missions are used in this study. SMOS data are obtained from the level 3 gridded product (Bitar et al., 2017) provided by the centre Aval de Traitement des Données SMOS (CATDS, <https://www.catds.fr>) operated for the centre National d'Etudes Spatiales (CNES) by the French Research Institute for Exploitation of the Sea (IFREMER). The data are available from 15

Table 1
 Perturbations associated with the forcing data and model parameters. The complete parameter description can be found in Decker (2015) and Ukkola et al. (2016).

Forcing/ parameter variables	Description	Spatially correlated	Perturbation type	Standard deviation
Meteorological forcings				
Rainf	Precipitation	Yes	Multiplicative	Obtained from Huffman (1997)
SW	Shortwave radiation	Yes	Multiplicative	10% of the nominal value
Tair	Air temperature	Yes	Additive	10% of the nominal value
Model parameters				
$f_{clay} f_{sand} f_{silt}$	The fraction of clay, sand, and silt	No	Multiplicative	10% of the nominal value
f_{sat}	The fraction of the grid cell that is saturated	No	Additive	10% of the nominal value
q_{sub}	The maximum rate of subsurface drainage assuming a fully saturated soil column	No	Additive	10% of the nominal value
f_p	Tunable parameter controlling drainage speed	No	Additive	10% of the nominal value

January 2010 to present, with a spatial resolution of ~25 km on the Equal-Area Scalable Earth (EASE; Brodzik et al., 2012) grid. The SMAP data are retrieved from the level 3 (version 4) radiometer global daily 36 km EASE-grid product (SPL3SMP) provided by the National Snow and Ice Data Center Distributed Active Archive Center (NSIDC DAAC, <https://nsidc.org/data/smap>). The product contains the volumetric soil moisture retrieved by the SMAP passive microwave radiometer, available from 31 March 2015 to present. For both SMOS and SMAP, the data are resampled to a 25 km regular grid to reconcile the observations with the model grid space. On days for which more than one SM retrieval is available, the daily average is used to ensure consistency with the model time step.

Following previous SM studies (e.g., Colliander et al., 2017; Lievens et al., 2015; Liu et al., 2016), the measurement error of both SMOS and SMAP are both assumed to be $0.04 \text{ m}^3/\text{m}^3$. It is acknowledged that triple collocation analysis (TCA) may potentially provide more accurate SM error estimates (De Lannoy and Reichle, 2016). However, applying TCA in SM DA requires linear consistency between modeled and retrieved SM (Dong and Crow, 2018). This assumption has not yet been validated in practice. Therefore, constant, rather than TCA-based, error estimates are used in this study.

The assimilation of satellite soil moisture data into the LSM requires the application of rescaling to reduce systematic bias that may be found between the model estimate and the observation (Crow et al., 2005; Reichle and Koster, 2004). The bias correction can be used to transform the observation into model space and reduce the inconsistency between their respective climatology (Koster et al., 2009; Renzullo et al., 2014). In this study, cumulative density function matching (CDF-matching; Reichle and Koster, 2004) is used to rescale satellite observation to LSM climatology. The approach is applied separately for each model grid cell, and each satellite data product (with respect to its entire period).

2.5. In situ data

The in situ soil moisture and groundwater measurements between January 2010 and December 2015 are obtained from the ground observation networks for validation. The in situ soil moisture data are provided by the SASMAS network (Rüdiger et al., 2007). Data at each depth are provided in terms of volumetric soil moisture (θ , m^3/m^3). The 0 – 5 ($\theta_{0-5\text{cm}}$) and 0 – 30 cm ($\theta_{0-30\text{cm}}$) data are used in this study due to their compatibility with the model soil layers (see Section 2.2). In situ groundwater level data (H) are obtained from the Department of Primary Industries (DPI), Office of Water, NSW (<http://www.water.nsw.gov.au>). Groundwater storage (GWS) simulated in the model can be converted to H if specific yield data are available. However, this is not the case for the Goulburn Catchment.

3. Methodology

3.1. Ensemble open-loop (EnOL)

The EnOL is used as a reference to evaluate the performance and the uncertainty of the LSM outputs. In the EnOL, the forcing data (\mathbf{u}) and model parameters (α) are perturbed (see Section 2.2), and the model propagation is performed without assimilation as:

$$\mathbf{x}_{i|t-1}^i = \mathbf{f}(\mathbf{x}_{i|t-1}^i, \mathbf{u}_t^i, \alpha^i), \quad (1)$$

where \mathbf{f} is the model operator used to propagate the states from $t - 1$ to t , \mathbf{x} is the model state vector, and $i = 1, 2, 3, \dots, N$ denotes the index of ensemble member (N in total). In this paper, the EnOL estimate is the ensemble mean of $\mathbf{x}_{i|t-1}^i$. Note that the perturbed initial states are obtained by spinning up the model (in EnOL mode) for six years (between 2004 and 2009) prior to the assimilation period. In this study, the state vector (\mathbf{x}) consists of a total of seven variables (soil moisture at six layers and one groundwater storage, see Section 3.2 for more details). The contribution of the snow water and canopy water components to the total water storage in the Goulburn catchment are negligible. Hence, they

are not included in the state vector. Following Tangdamrongsub et al. (2017a), an ensemble size of $N = 300$ is used, which is sufficient to ensure the effectiveness of DA in the Goulburn catchment.

3.2. Ensemble Kalman smoother (EnKS)

The EnKS consists of a forecast and analysis (update) step. Similar to the EnOL, the states are propagated forward in time using the LSM in the forecast step. The period of model propagation depends on the period of the assimilated observations (e.g., approximately one month for GRACE). A set of observations was computed by perturbing the measurement with its associated covariance \mathbf{R}_s (Burgers et al., 1998). The subscript s denotes smoother, e.g., $s = t - L + 1 : t$ where L is the smoother window length. The state vector is updated as:

$$\mathbf{x}_{s|s}^i = \mathbf{x}_{s|t-L}^i + \mathbf{K}_s (\mathbf{y}_s^i - \mathbf{H}_s \mathbf{x}_{s|t-L}^i) \quad (2)$$

with

$$\mathbf{K}_s = \mathbf{P}_{e,s} \mathbf{H}_s^T (\mathbf{H}_s \mathbf{P}_{e,s} \mathbf{H}_s^T + \mathbf{R}_{e,s})^{-1} \quad (3)$$

where \mathbf{y}_s^i is a perturbed observation vector, \mathbf{H}_s is an operator which relates the ensemble state $\mathbf{x}_{s|t-L}^i$ to the measurement vector \mathbf{y}_s^i , \mathbf{K} is the Kalman gain matrix, and $\mathbf{P}_{e,s}$ and $\mathbf{R}_{e,s}$ are the ensemble error covariance matrices of the model and observation, respectively. Note that the state variables from $t - L + 1$ to t are considered in the smoother case. If the matrix \mathbf{A} contains the ensemble states and $\bar{\mathbf{A}}$ is the matrix of the same size as \mathbf{A} and filled with the mean value computed from all ensemble members, the ensemble error covariance matrix $\mathbf{P}_{e,s}$ can be computed as follows:

$$\mathbf{P}_{e,s} = (\mathbf{A} - \bar{\mathbf{A}})(\mathbf{A} - \bar{\mathbf{A}})^T / (N - 1). \quad (4)$$

Similarly, \mathbf{R}_e is computed as:

$$\mathbf{R}_{e,s} = (\mathbf{D} - \bar{\mathbf{D}})(\mathbf{D} - \bar{\mathbf{D}})^T / (N - 1), \quad (5)$$

where \mathbf{D} stores the perturbed observation and $\bar{\mathbf{D}}$ is the ensemble mean. The DA estimate is the ensemble mean of $\mathbf{x}_{s|s}^i$.

3.3. Design of the DA schemes

The different DA schemes are developed to incorporate observations with different spatial-temporal resolutions and error characteristics into the DA system simultaneously. Three different DA schemes are considered here (Fig. 2), SM DA (only soil moisture is assimilated), GRACE DA (only GRACE is assimilated), and multivariate DA (both soil moisture and GRACE are assimilated).

As described in Section 3.2, the state vector contains daily volumetric soil moisture of six different layers and groundwater storage components. For a particular model grid cell (j) on a given day (t), the state vector can be defined as $[\theta_1^{j,t} \ \theta_2^{j,t} \ \theta_3^{j,t} \ \theta_4^{j,t} \ \theta_5^{j,t} \ \theta_6^{j,t} \ gws^{j,t}]^T$, where θ is the volumetric soil moisture (m^3/m^3), and gws is the groundwater storage (m). The state variables are obtained from the results of model propagation.

In the SM DA (Fig. 2a), the soil moisture observations are assimilated every $L = 3$ days on the model grid cell individually. Only SMOS data is used between January 2010 and February 2015, and the dimension of the state vector is $ML \times 1$, where $M = 7$ is the number of the state variables. The 3-day window allows the soil moisture observations to have full coverage over the Goulburn catchment and yields the adequate ensemble spread between the updates. The observation vector \mathbf{d} contains the SMOS data with dimension $L \times 1$. The \mathbf{H}_s matrix is defined as:

$$\mathbf{H}_s = \begin{bmatrix} \mathbf{h}_{SM}^{j,t=1} & 0 & 0 \\ 0 & \mathbf{h}_{SM}^{j,t=2} & 0 \\ 0 & 0 & \mathbf{h}_{SM}^{j,t=3} \end{bmatrix} \quad (6)$$

$$\mathbf{h}_{SM}^{j,t} = [s_1 \ s_2 \ 0 \ 0 \ 0 \ 0 \ 0], \quad (7)$$

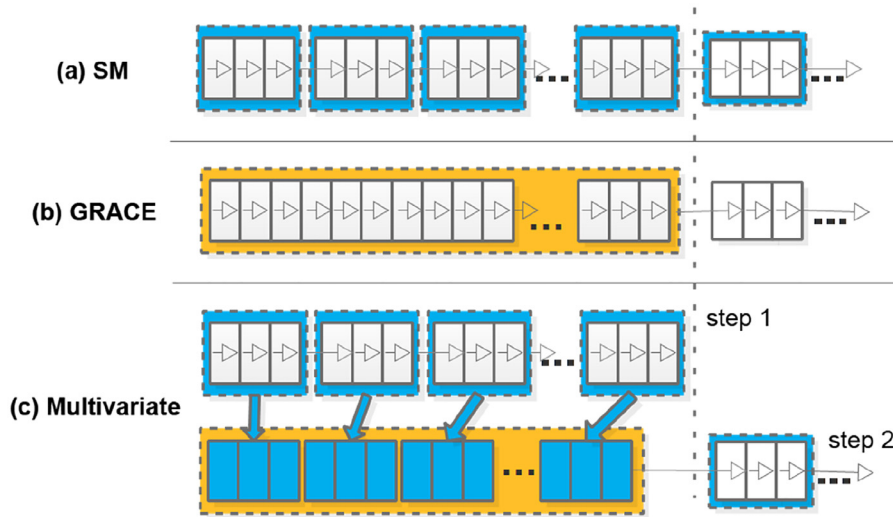


Fig. 2. Three different DA schemes, SM-only DA, GRACE-only DA, and multivariate DA. The SM DA (a) updates the state estimate using the time window of approximately three days (blue rectangle in (a)) while the GRACE DA (b) uses the time window of approximately one month (orange rectangle in (b)). In the multivariate DA (c), the SM DA is first performed (step 1 in (c)), and its updated states are used as the forecast state in the GRACE DA (step 2 in (c)). (For interpretation of the references to color in this figure legend, the reader is referred to the web version of this article.)

where s_1, s_2 are the thickness of the first and second soil layers, respectively. The soil thickness is described in Section 2.2. The H_s matrix (dimension $L \times ML$) relates the SMOS observation to the top two soil layers. Bias correction is performed prior to the application of DA to reduce the systematic error between the model estimated and the satellite retrieved soil moisture (see Section 3.3). When SMAP data are available, e.g., from March 2015, the SMOS and SMAP data are assimilated into the LSM, simultaneously. Lievens et al. (2017) demonstrated that the joint SM DA performed better than a single SM DA case. In the case of SMOS/SMAP assimilation, the dimension of H_s and d are extended to $2L \times ML$, and $2L \times 1$, respectively, to include the measurement operator associated with the SMAP data. In this study, the errors in SMOS and SMAP data are assumed to be uncorrelated.

In the GRACE DA (Fig. 2b), the model states are updated at a monthly time scale consistent with the GRACE temporal resolution. The model state vector contains all model grid cells (inside the blue polygon in Fig. 1) of daily state variables within approximately one month. The state vector is also constructed from the results of model propagation. The length of the vector is JLM , where J is the number of grid cells in the study area, and $L \approx 1$ month. The monthly time window used for each update is based on the time tag of the GRACE product. As the monthly window used to produce a GRACE solution is not necessarily a calendar month, L is different in each update and varies between 13 and 31 days (following GRACE data used). The observation vector y_s is a 1×1 vector containing the monthly average values of the catchment mean TWS. The matrix H_s is used to convert the volumetric soil moisture and groundwater storage into the catchment averaged TWS of the month:

$$H_s = [h_G^{i=1} \quad h_G^{i=2} \quad \dots \quad h_G^{i=L}] \quad (8)$$

$$h_G = [g^{j=1} \quad g^{j=2} \quad \dots \quad g^{j=J}] \quad (9)$$

$$g^j = [s_1 \quad s_2 \quad s_3 \quad s_4 \quad s_5 \quad s_6 \quad 1] / JLL, \quad (10)$$

where $s_1 - s_6$ are the thickness of each soil layer (see Section 2.2).

In the multivariate DA (Fig. 2c), the SM DA and GRACE DA schemes are combined. The SM DA is firstly performed (step 1 in Fig. 2c), and its updated state variables are used as the forecast state in the GRACE DA (step 2).

It should be noted that, unlike the 3D EnKF (Reichle and Koster, 2003), satellite soil moisture observations are only used for correcting collocated soil moisture estimates. However, a recent study demonstrates that remote sensing observation error is highly structured in space – suggesting a spatial correlation of soil moisture retrieval errors

(Dong et al., 2017). This complicates the accurate parameterization of the observation error matrix in a 3D updating DA scheme. Hence, the soil moisture retrievals are not used for correcting nearby grid cells.

3.4. Evaluation metrics

The volumetric soil moisture estimates are validated with the in situ soil moisture and groundwater data in terms of temporal correlation (ρ), and unbiased root mean square difference (ubRMSD; Entekhabi et al., 2010):

$$\rho = \frac{\sum (x_{sim} - E[x_{sim}])(x_{obs} - E[x_{obs}])}{\sqrt{\sum (x_{sim} - E[x_{sim}])^2 \sum (x_{obs} - E[x_{obs}])^2}} \quad (11)$$

$$ubRMSD = \sqrt{E\{[(x_{sim} - E[x_{sim}]) - (x_{obs} - E[x_{obs}])]^2\}} \quad (12)$$

where x_{sim} and x_{obs} are state vectors from simulation (model estimate) and observation (e.g., satellite product, in situ data), respectively, and $E[\cdot]$ is the expectation operator.

All in situ soil moisture and groundwater data inside the same model grid cell (Fig. 1) are averaged before the comparison. This produces four grid cells of in situ soil moisture (S1 – S4) and four of in situ groundwater data (G1 – G4). Note that, only the temporal correlation between H and GWS is used to evaluate the groundwater storage estimate (against groundwater level) due to the absence of accurate information on specific yield.

4. Results and discussion

4.1. Impact of DA on soil moisture estimate

The top soil moisture (θ_{0-5cm}) is estimated from the EnOL and three DA scenarios (SM-only, GRACE-only, and both). The goodness of fit in terms of correlation is evaluated against the SMOS data (Fig. 3, top row) to investigate the impact of different DA scenarios on the θ_{0-5cm} estimates. From Fig. 3, the SM DA and the multivariate DA deliver $\sim 0.1 - 0.15$ higher averaged correlation values compared to the EnOL. This is expected, as the SMOS/SMAP data are being integrated into the state estimate (particularly into the θ_{0-5cm} component) by the applications of the SM DA and multivariate DA. The Kalman gain attempts to statistically optimize the fit between the θ_{0-5cm} estimate and the SMOS/SMAP observation, resulting in an improved agreement between them. Similar behavior is also observed from the evaluation with the SMAP data (not shown). Including the SMOS/SMAP data in the assimilation system is proven necessary to improve the θ_{0-5cm} estimate.

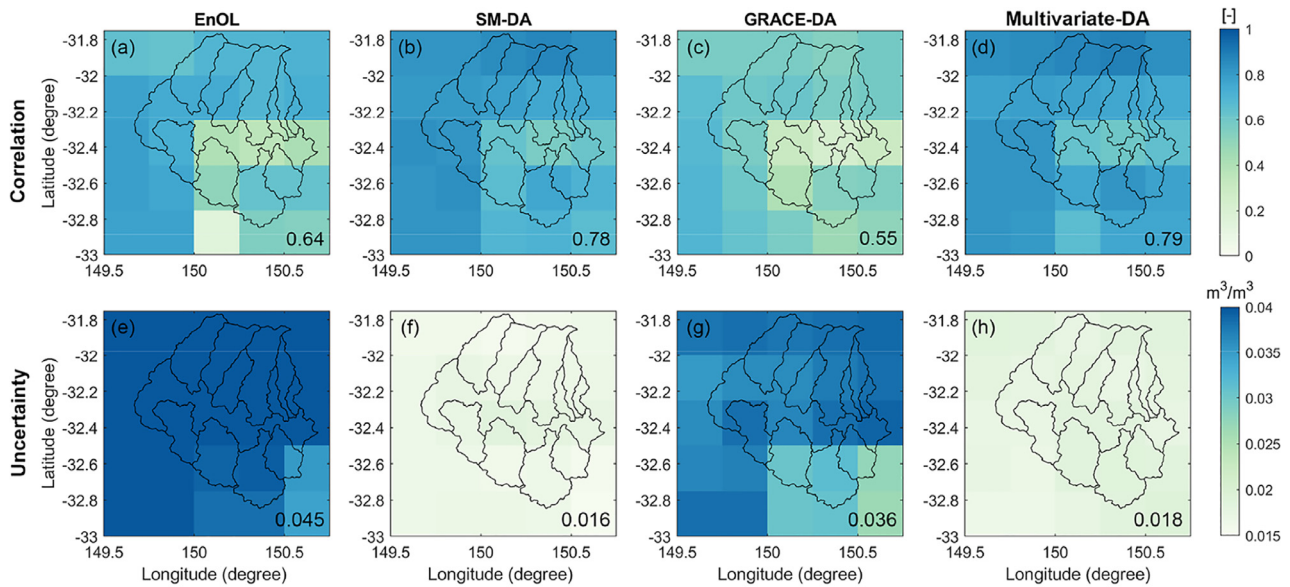


Fig. 3. The correlation coefficients (top row) and uncertainty (ensemble spread, bottom row) of the 0 – 5 soil moisture estimates computed between the SMOS data and different DA case studies. The averaged correlation and error values of the Goulburn catchment are given in each figure.

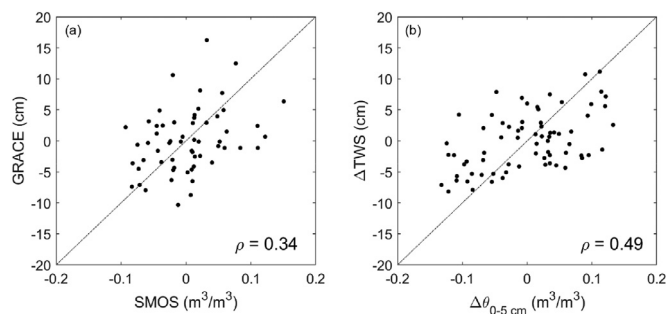


Fig. 4. Scatter plots between the basin-averaged Δ TWS and soil moisture anomaly ((a) GRACE Vs. SMOS, and (b) CABLE-estimated Δ TWS and $\Delta\theta_{0-5cm}$) of the Goulburn catchment. The correlation coefficient (ρ) is provided in each figure.

By contrast, GRACE DA reduces the correlation value by ~ 0.1 . The degradation is likely caused by the limited sensitivity of GRACE observations to top soil moisture. The top soil component is strongly governed by high-frequency meteorological forcing (Wu et al., 2002) while GRACE can only observe monthly catchment-averaged TWS changes, which is dominated by the low-frequency variability of deep-water storage components. Also, the degradation of surface SM after assimilating GRACE suggests an inconsistency between the observed and modeled SM-TWS relationship. As shown in Fig. 4, the modeled TWS change is less sensitive to the modeled SM change, compared to the corresponding observations. Therefore, correcting the modeled TWS to GRACE may over-correct SM estimates and lead to degraded results. Clearly, assimilating GRACE data alone cannot provide the high spatiotemporal variability essential for modeling the water storage in the top soil layer, and the inclusion of GRACE data tends to have a negative impact on the θ_{0-5cm} estimate.

All DA cases reduce the uncertainty (ensemble spread) of the θ_{0-5cm} estimate (Fig. 3, bottom row). Compared to the EnOL, the SM DA and multivariate DA reduce the uncertainty by a factor of three while the GRACE DA reduces the uncertainty by a factor of 1.2. Importantly, the applications of the SM DA and multivariate DA also lead to an approximately three times lower uncertainty than the assigned SMOS/SMAP uncertainty value. In addition, it is seen that the uncertainty of the θ_{0-5cm} estimate is lower in the south-eastern part of the catchment. This is likely

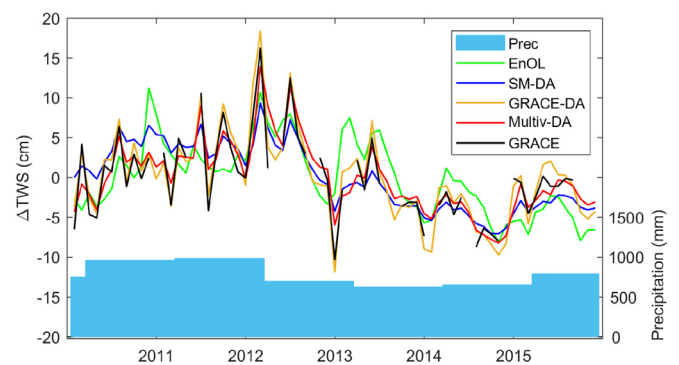


Fig. 5. The monthly basin-averaged Δ TWS computed from different DA approaches (SM DA, GRACE DA, and multivariate DA). The EnOL estimate, the GRACE observation, and the yearly precipitation accumulated between April and May are also shown for comparison.

influenced by the lower field capacity associated with lower clay content in the southern region, leading to a small variation of θ_{0-5cm} and its uncertainty. The spatial pattern of the uncertainty also explains the contribution of SMOS/SMAP observation. The update is likely limited in the south-eastern part where the model uncertainty is small. This is apparent in, e.g., Fig. 3b where slightly lower correlation values are observed mostly in the south-eastern region.

4.2. Impact of DA on TWS estimate

The basin-averaged Δ TWS of all three DA cases is shown in Fig. 5. Also, the correlation with respect to GRACE is shown in Fig. 6 (top row). Assimilating SMOS/SMAP only yields a negative impact on the Δ TWS estimates, resulting in a decreased agreement between the state estimate and the GRACE observation. In the SM DA, the smoother underestimates the annual and inter-annual variability of Δ TWS and reduces the averaged correlation value by ~ 0.2 (Fig. 6b). The smoothers estimate a set of the ensemble by optimizing the Kalman gain (or likelihood) function associated only with the θ_{0-5cm} component while leaving the other storage components unconstrained. Computing the posterior estimate based on the resulted sample set produces an improved θ_{0-5cm} estimate (see also Section 4.1), but does not necessarily improve the computation of

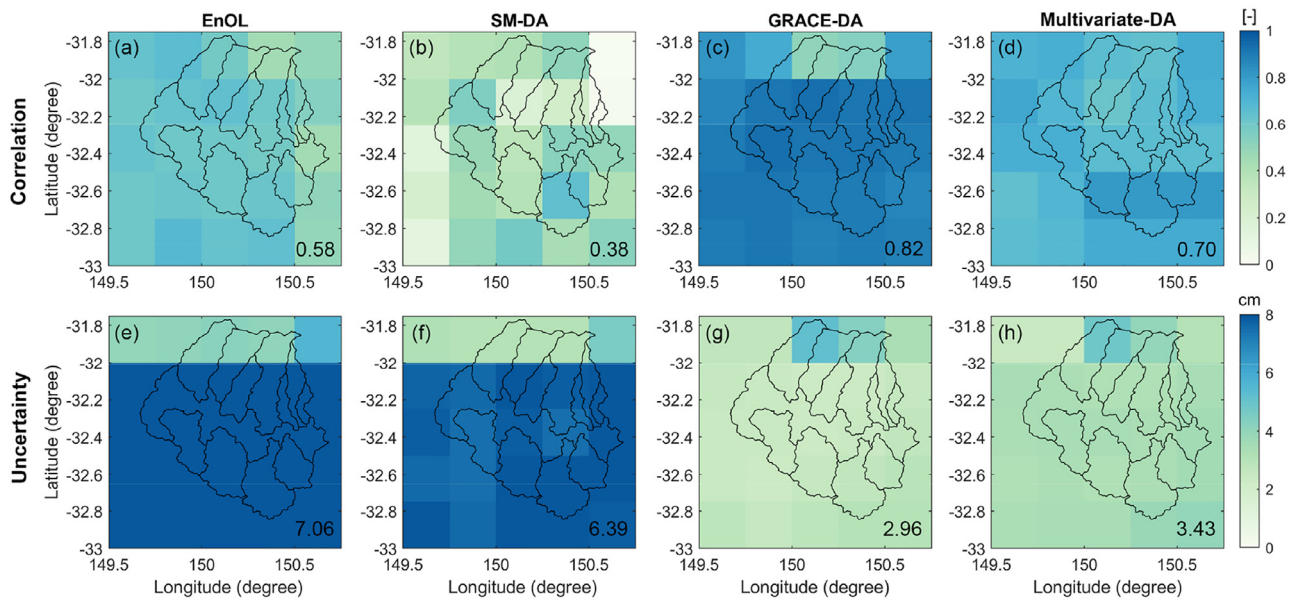


Fig. 6. The correlation coefficients (top row) and errors (ensemble spread, bottom row) of the Δ TWS estimate computed between the GRACE observation and different DA case studies. The averaged correlation and error values of the Goulburn catchment are given in each figure.

Table 2

Total mass variations (Gton) estimated from nine different DA case studies, model estimate (EnOL), and GRACE observation during two periods: January 2010 – March 2012 and April 2012 – December 2015.

Period	SM DA	GRACE DA	Multivariate DA	EnOL	GRACE observation
Jan 2010 – Mar 2012	0.12	0.64	0.56	0.48	0.61
Apr 2012 – Dec 2015	-0.21	-0.30	-0.34	-0.47	-0.35

total storage changes. The degradation in Δ TWS may be due to the fact that the satellite SM observation does not provide information on the total column water, which is crucial in the accurate distribution of the water through all stores.

In the GRACE DA, the constraint is applied to the entire water column, leading to an improved agreement between the Δ TWS estimate and the GRACE observation. The averaged correlation value is increased by ~ 0.2 (Fig. 6c). The impact of the GRACE DA is clearly seen in the Δ TWS adjustment before and after March 2012. To evaluate this, the total mass variation in the two periods (January 2010 – March 2012 and April 2012 – December 2015) is computed and shown in Table 2. To determine the total mass of TWS variation (Gton) in each period, the long-term trend (m/year) is first estimated, and multiplied by the area of the Goulburn catchment (see Section 2.1), the density of water, and the number of years in that period, respectively. GRACE observes the increased mass estimate of ~ 0.6 Gton prior to April 2012, which is mainly induced by the 2010 – 2011 La Niña rainfall (see Fig. 5). The EnOL underestimates the mass estimate by ~ 0.1 Gton during this period. The estimate is improved by the GRACE DA, leading to a $\sim 20\%$ improvement in cross-correlation between the adjusted mass estimate and GRACE data. Similar behavior is observed during the post La Niña period (after March 2012) when the GRACE DA produces a $\sim 30\%$ improvement in cross-correlation. Unlike the GRACE DA, the SM DA cannot improve the mass estimate in both periods due to e.g., the deficiency of deep-water storage information necessary for the TWS computation.

It is apparent that SM DA and GRACE DA are valuable for updating $\theta_{0-5\text{cm}}$ and TWS estimates, respectively, while they show limited benefit for the estimation of the other components. The underlying strengths motivate the concept of assimilating the SMOS/SMAP and GRACE observation simultaneously into the LSM. In the multivariate DA, the $\theta_{0-5\text{cm}}$ and Δ TWS components are adjusted toward the SMOS/SMAP and GRACE observation, respectively, resulting in the fi-

nal state estimates that agree with both observations. The Δ TWS estimated with multivariate DA agrees better with the GRACE observations by ~ 0.12 in cross-correlation (Fig. 6d) and, simultaneously, the $\theta_{0-5\text{cm}}$ estimate presenting better correlation by >0.1 with SMOS/SMAP data (see Fig. 3b). Consequently, the multivariate DA improves the mass estimate during the La Niña period (Table 2).

The GRACE DA and multivariate DA reduce the TWS uncertainty by more than a factor of 2 (Fig. 6, bottom row). As expected, the SM DA cannot deliver a reliable TWS estimate, as seen in the uncertainty which is approximately twice that obtained from the GRACE DA and multivariate DA.

4.3. Validation with in situ data

4.3.1. Soil moisture

The $\theta_{0-5\text{cm}}$ variations estimated from all DA case studies are validated against the in-situ data at S1 – S4 (Fig. 7). The validation is conducted in terms of correlation and ubRMSD, and the estimated values are shown in Fig. 8. CABLE performs remarkably well in the estimation of $\theta_{0-5\text{cm}}$, and provides a good agreement with the in situ data at all locations with an averaged correlation value of ~ 0.69 (see EnOL in Fig. 8a). The SM DA and multivariate DA increase the correlation value further by $\sim 7\%$ (from ~ 0.69 to ~ 0.73) and decrease the ubRMSD by $\sim 11\%$. The improved result is anticipated since the satellite SM observation is used in the SM DA and multivariate DA. By contrast, the GRACE DA shows an apparent negative impact on the $\theta_{0-5\text{cm}}$ estimate (see, Fig. 8a, b). Comparing to the EnOL, the GRACE DA overestimates $\theta_{0-5\text{cm}}$ by a factor of 1.5 (ubRMSD), and decreases the correlation by 50%. Poor performance is due to the insensitivity of GRACE data to the signal associated with the top soil component as described in Sections 4.1 and 4.2.

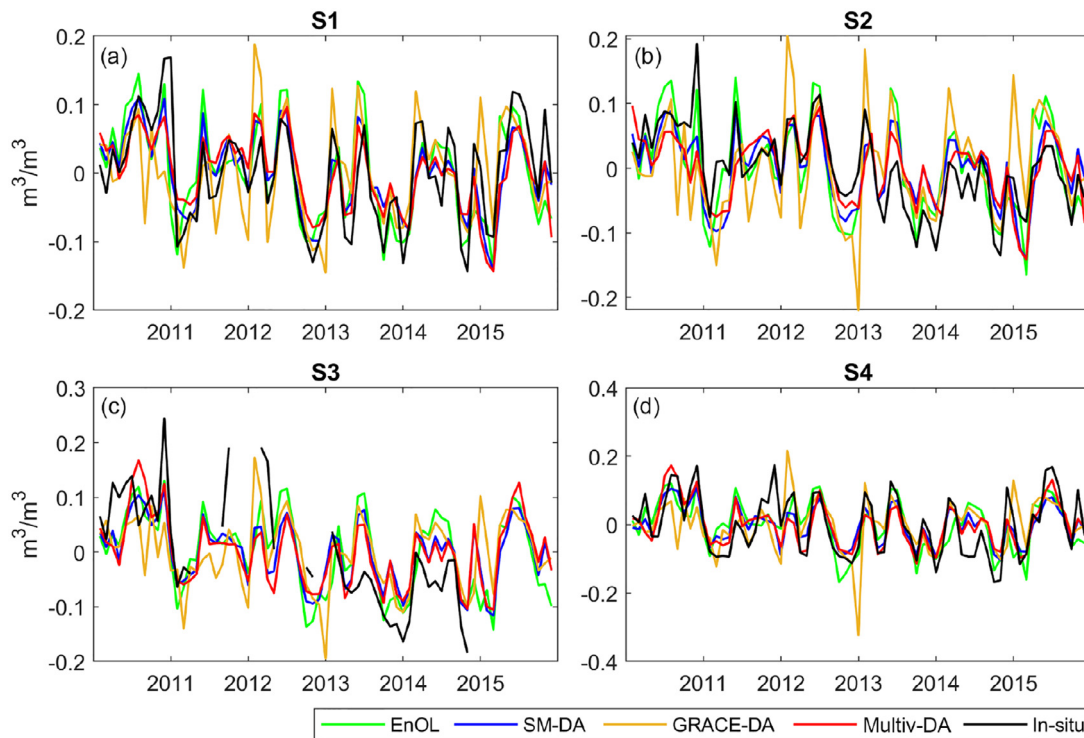


Fig. 7. The monthly “0 – 5 cm” soil moisture variations estimated at S1 – S4 pixels computed from different DA approaches (SM DA, GRACE DA, and multivariate DA). The EnOL estimates and the in situ soil moisture data are also shown for comparison.

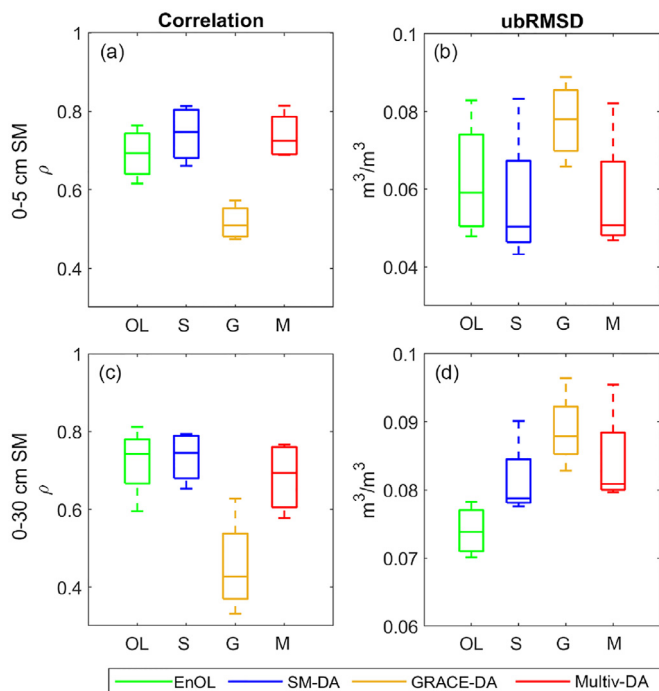


Fig. 8. The correlation coefficients (a, c) and unbiased root mean square differences (ubRMSD; b, d) of the 0 – 5 cm soil moisture (top row) and 0 – 30 cm soil moisture (bottom row) computed from the estimate of different DA case studies at S1 – S4 (S: SM DA, G: GRACE DA, M: Multivariate DA). The statistical results of the EnOL (OL) are also shown.

The $\theta_{0-30\text{cm}}$ variation is also validated against the in-situ data with the statistical results shown in Fig. 8 (bottom row). CABLE provides a very accurate $\theta_{0-30\text{cm}}$ component with a correlation value of almost 0.7 (Fig. 8c). Unlike the $\theta_{0-5\text{cm}}$, the SM DA and multivariate DA do not improve the correlation and ubRMSD values of the $\theta_{0-30\text{cm}}$ estimate. This is consistent with previous studies that found that the benefit of surface SM DA in root zone SM estimates depends on the accuracy of model physics (Dunne et al., 2007; Kumar et al., 2009). In line with the analysis found in Fig. 4, GRACE DA also reduces the quality of the $\theta_{0-30\text{cm}}$ estimate, seen from both metrics.

The benefit of including the SMAP data in the DA system is evaluated. The multivariate DA results from two case studies using SMAP data between March and December 2015 are compared with the in-situ data at S1, S2, and S4 (Fig. 9a – c). The in-situ data at S3 are not available during this validation period. In all locations, the daily $\theta_{0-5\text{cm}}$ estimates of the SMOS-only assimilation and the SMOS/SMAP assimilation are very similar and visibly show a better agreement with the in-situ data (comparing to the EnOL). The correlation value is increased to almost 0.2 (e.g., at S1, Fig. 9d), and the highest correlation value is seen when the SMAP data is included in the DA system (~3% higher compared to the SMOS-only assimilation). The application of the SMOS/SMAP assimilation also reduces the spurious peaks of the $\theta_{0-5\text{cm}}$ estimate, e.g., in October 2015 (Fig. 9a, b) and November 2015 (Fig. 9c), leading to a better agreement with the in-situ data. Evidently, the SMAP data should be considered in the DA process to maintain the accuracy (in terms of agreement with the in situ data) of the $\theta_{0-5\text{cm}}$ estimate in the Goulburn catchment.

4.3.2. Groundwater storage

The ΔGWS estimates are compared with the in-situ groundwater level anomalies (ΔH) at G1 – G4 (Fig. 10), and the averaged correlation coefficients are shown in Fig. 11. In Fig. 10, the application of the SM DA leads to an incorrect groundwater storage estimate with a large disagreement between the ΔGWS estimate and ΔH , particularly at G1 where the correlation value is as low as -0.6 . The poor performance

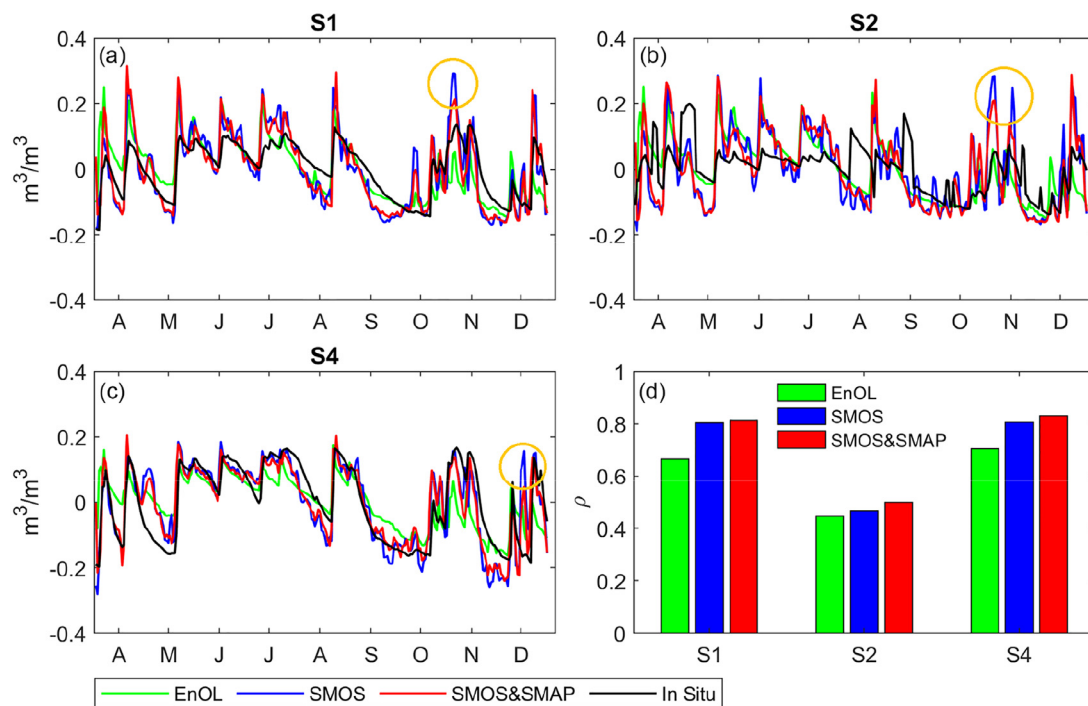


Fig. 9. The daily 0–5 soil moisture variations estimated at S1 (a), S2 (b), and S4 (c) pixels from the EnOL estimate, the SMOS-only DA estimate, the SMOS/SMAP DA estimate, and the in situ data between March and December 2015. Circles indicate the spurious peaks found in SMOS-only DA estimate. The correlation coefficients between the in situ data and the results of the EnOL, the SMAP-only DA, and the SMOS/SMAP DA are shown in (d).

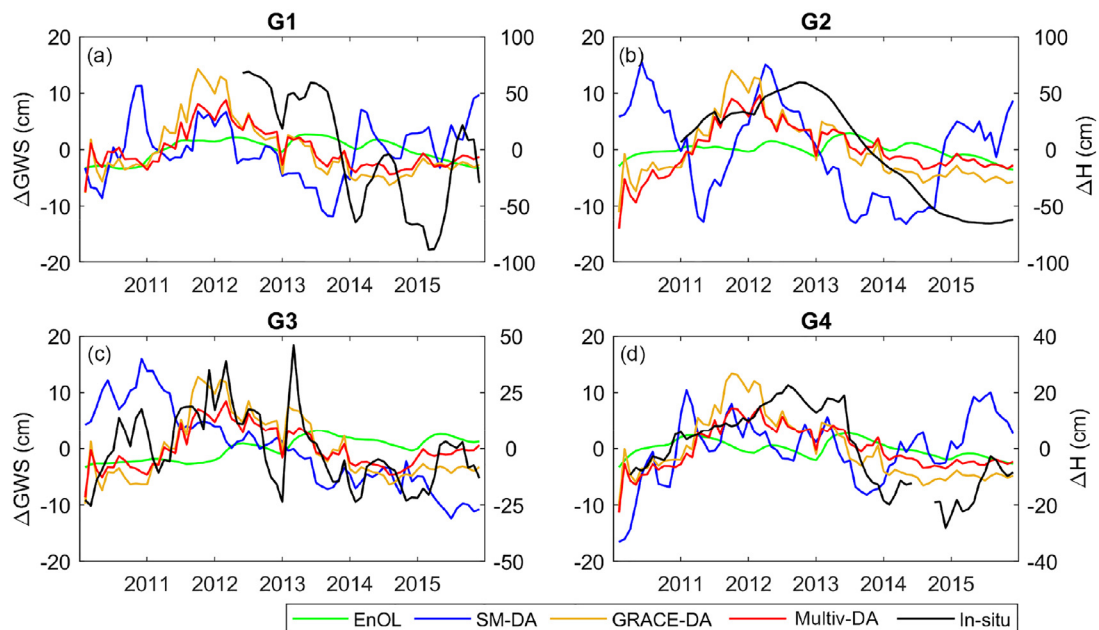


Fig. 10. The monthly groundwater storage variations (ΔGWS) at G1 – G4 pixels computed from different DA approaches (SM DA, GRACE DA, and multivariate DA). The EnOL estimates and the in situ groundwater level variations (ΔH) are also shown for comparison.

can be attributed to the lack of groundwater information in the satellite SM observation (see Sections 4.1 and 4.2). The ΔH shows a very similar temporal variation in all G1 – G4 locations. The different scale between ΔGWS and ΔH likely causes the visual phase shift seen in Fig. 10. Applying a specific yield (e.g., ranging between 0 and 1) to ΔH could reduce the magnitude of the right axis, and led to the reduction of visual phase shift. However, the conversion is not performed due to the absence of specific yield as described in Section 2.5. The temporal variations of ΔH follow those of the ΔTWS estimate and the GRACE observations (see

Fig. 5). ΔH (and ΔTWS) increases under the influence of the La Niña rainfall in 2011 – 2012 and decreases afterward. The similarity suggests that GRACE is sensitive to the signal of the groundwater store more than the shallow storage component. In particular, the groundwater level data (ΔH) are correlated throughout the catchment with the cross-correlation of ~ 0.9 (see Fig. 6 in Tangdamrongsub et al. (2017a)). The assimilation of GRACE data (in both GRACE DA and multivariate DA) increases the correlation between the ΔGWS estimate and ΔH changes in each grid by a factor of 2, compared to the EnOL estimate.

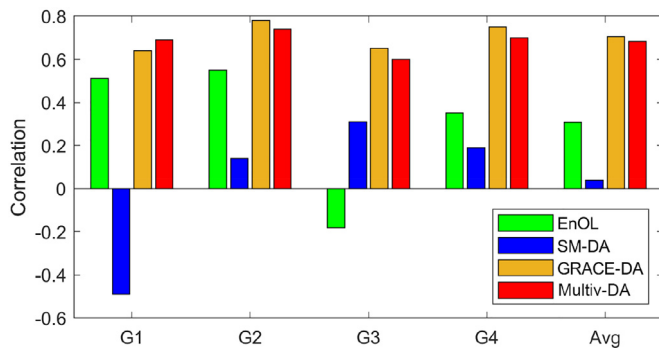


Fig. 11. The correlation coefficients of the Δ GWS estimates at (a) G1, (b) G2, (c) G3, and (d) G4 pixels computed from EnOL and different DA case studies. The averaged correlation values (Avg) of G1 – G4 are also shown.

The EnOL-simulated Δ GWS shows smaller variations compared to the DA estimate and Δ H. CABLE models the unconfined aquifer using a simple groundwater model (Decker, 2015; Decker and Zeng, 2009; Niu et al., 2007; Vergnes et al., 2012) that calculates the groundwater recharge based on the available water after vertical redistribution between the soil layers. This simplification might lead to an enclosed groundwater component in the deep soil layer when the distributing water does not reach the defined field capacity. In such a case, groundwater recharge is not accounted for correctly, and the groundwater storage changes become small. The soil and groundwater components are not efficiently separated, and the variation of the Δ GWS estimate is likely presented in the deep soil layer.

Assimilating GRACE-only always shows a better performance in the Δ GWS estimate and provides ~29% higher average correlation compared to assimilating both GRACE and SMOS/SMAP measurements. In the multivariate DA, Δ GWS is updated by the GRACE DA (step 2 in Fig. 2c) after the application of the SM DA (step 1 in Fig. 2c). The application of the SM DA (in the multivariate DA) likely decreases the uncertainty of the state estimate, which consequently reduces the contribution of GRACE in the analysis step of the GRACE DA. Rescaling the GRACE uncertainty could increase the contribution of the GRACE observation (e.g., Tian et al., 2017).

5. Conclusions

This study evaluates three different DA schemes to assimilate different combinations of satellite observations (SMOS/SMAP, GRACE, and both (SMOS/SMAP and GRACE)) in the Goulburn catchment, Australia. Validation against the in-situ data reveals that the performance of the DA in estimating soil moisture and groundwater storage highly depends on the choice of the observation type. The application of the SM DA significantly improves the top (0 – 5 cm) soil moisture but degrades the groundwater component, whereas the GRACE DA improves only the Δ GWS estimate. Applying the multivariate DA simultaneously increases the accuracy of the soil moisture and groundwater storage estimates, though at a slightly lesser degree of improvement compared to the single observation DA case.

The application of the SM DA underlines the importance of the SMOS/SMAP data on the SM estimate, by increasing the 0 – 5 cm correlation with in situ observations by up to 7%. The benefit on the 0 – 30 cm soil moisture and groundwater component is minor or negative, which is in line with several previous studies. For example, Blankenship et al. (2016), Kolassa et al. (2017), Ridler et al. (2014) and Tian et al. (2017), who reported a detrimental impact on the root zone and deep storage components. SM DA significantly reduces the uncertainty of storage in the top 0 – 5 cm soil layer but does not have an impact on the TWS uncertainty. The constraint solely in the top soil moisture component by the SM DA does not necessarily have a positive effect on the entire wa-

ter column. We also found that assimilating both SMOS and SMAP data simultaneously is recommended in the Goulburn catchment. The advantage of multivariate SM DA is also found in Lievens et al. (2017), Kumar et al. (2018), Jasinski et al. (2019). However, it should be noted that SMOS and SMAP soil moisture may have potentially common systematic errors, which may affect the observation error matrix. Future studies should explore the magnitude of SMOS-SMAP error cross-correlation and its impact on the DA results.

The GRACE DA demonstrates an outstanding example of improving the groundwater storage of the Goulburn catchment, particularly at a finer spatial resolution (~25 km) compared to GRACE's intrinsic resolution (>100 km). As the groundwater variation of the Goulburn catchment is likely to be spatially correlated due to the large unconfined aquifer (Tangdamrongsub et al., 2017a), assimilating a coarser spatial scale Δ TWS from the GRACE observation can benefit the groundwater estimate even in the smaller individual grid cell. GRACE DA leads to the improved groundwater estimate by increasing the correlation to independent in situ groundwater level data. However, assimilating GRACE into LSM does not provide a positive impact on the top or surface SM components. This is consistent with the conclusions of Li et al. (2012) and Tian et al. (2017). GRACE DA significantly reduces the uncertainty of the TWS estimate but has only a minor impact on the SM uncertainty. It is known that GRACE is sensitive to the signal of the entire water column, dominated by the processes in deeper layers. The GRACE DA might therefore adversely distribute the deep water storage signals into the shallow one.

Multivariate DA provides an improvement over both SM and Δ GWS estimates. Assimilating the satellite soil moisture and GRACE data together allows the high-frequency components to be adjusted by the SM DA while the low-frequency signal is corrected by the GRACE DA, leading to the increased correlation values of both the 0 – 5 cm soil moisture (by ~7%) and Δ GWS estimates (by ~65%), compared to the independent in situ data. However, the multivariate DA does not outperform the SM DA or the GRACE DA in the separate estimation of the “0 – 5 cm” soil moisture and Δ GWS. The DA approach optimized the model states with multiple cost functions relevant to shallow and deep groundwater storage changes (e.g., minimizing the residuals against both SMOS/SMAP and GRACE), resulting in an optimal solution that is not closer to one particular observation, as also found by Tian et al. (2017).

With the increased availability of satellite retrievals and ground measurement networks, multivariate DA can be an effective tool to exploit diverse observations. The multivariate DA presented in this study can be extended to include different types of new observations (e.g., soil moisture from Sentinel-1 (Lievens et al., 2017), Δ TWS from GRACE Follow-On (Flechtner et al., 2014), snow water equivalent from SnowEx (Kim, 2017)) with simple modification of the measurement operator as described in Section 3.2. Ongoing research is focused on the sensitivity to the selected window length (L) of the smoother (Dong et al., 2015) and applications over regions with different climate conditions (e.g., snow-covered basins).

Declaration of competing interest

None.

CRedit authorship contribution statement

Natthachet Tangdamrongsub: Conceptualization, Methodology, Software, Validation, Writing - original draft. **Shin-Chan Han:** Supervision, Writing - review & editing. **In-Young Yeo:** Resources, Writing - review & editing. **Jianzhi Dong:** Methodology, Writing - review & editing. **Susan C. Steele-Dunne:** Methodology, Writing - review & editing. **Garry Willgoose:** Resources. **Jeffrey P. Walker:** Writing - review & editing.

Acknowledgment

This work was funded by The University of Newcastle to support NASA's GRACE and GRACE Follow-On projects as an international science team member, and by the Australian Research Council Discovery Project (DP170102373). Natthachet Tangdamrongsub was supported by the NASA Earth Science Division in support of the National Climate Assessment. We thank AWR's associated editor and three anonymous reviewers who provided insightful and constructive comments, leading to a significant improvement of the paper. Data used in this study are publicly available with the access information provided in Section 2.

References

- Andreadis, K.M., Lettenmaier, D.P., 2006. Assimilating remotely sensed snow observations into a macroscale hydrology model. *Adv. Water Resour.* 29, 872–886. <https://doi.org/10.1016/j.advwatres.2005.08.004>.
- Bettadpur, S., 2012. Gravity recovery and climate experiment utcsr level-2 processing standards document for level-2 product release 0005. Center For Space Research. The University of Texas at Austin, USA.
- Bitar, A.A., Mialon, A., Kerr, Y.H., Cabot, F., Richaume, P., Jacqueline, E., Quesney, A., Mahmoodi, A., Tarot, S., Parrons, M., Al-Yaari, A., Pellarin, T., Rodriguez-Fernandez, N., Wigneron, J.-P., 2017. The global SMOS level 3 daily soil moisture and brightness temperature maps. *Earth Syst. Sci. Data* 9, 293–315. <https://doi.org/10.5194/essd-9-293-2017>.
- Blankenship, C.B., Case, J.L., Zavadsky, B.T., Crosson, W.L., 2016. Assimilation of SMOS retrievals in the land information system. *IEEE Trans. Geosci. Remote Sens.* 54, 6320–6332. <https://doi.org/10.1109/TGRS.2016.2579604>.
- Brodzik, M.J., Billingsley, B., Haran, T., Raup, B., Savoie, M.H., 2012. EASE-Grid 2.0: incremental but significant improvements for earth-gridded data sets. *ISPRS Int. J. Geo-Inf.* 1, 32–45. <https://doi.org/10.3390/ijgi1010032>.
- Burgers, G., Jan van Leeuwen, P., Evensen, G., 1998. Analysis scheme in the ensemble Kalman filter. *Mon. Weather Rev.* 126, 1719–1724. [https://doi.org/10.1175/1520-0493\(1998\)126<1719:ASITEK>2.0.CO;2](https://doi.org/10.1175/1520-0493(1998)126<1719:ASITEK>2.0.CO;2).
- Chan, S.K., Bindlish, R., O'Neill, P.E., Njoku, E., Jackson, T., Colliander, A., Chen, F., Burgin, M., Dunbar, S., Piepmeier, J., Yueh, S., Entekhabi, D., Cosh, M.H., Caldwell, T., Walker, J., Wu, X., Berg, A., Rowlandson, T., Pacheco, A., McNairn, H., Thibeault, M., Martínez-Fernández, J., González-Zamora, Á., Seyfried, M., Bosch, D., Starks, P., Goodrich, D., Prueger, J., Palecki, M., Small, E.E., Zreda, M., Calvet, J., Crow, W.T., Kerr, Y., 2016. Assessment of the SMAP passive soil moisture product. *IEEE Trans. Geosci. Remote Sens.* 54, 4994–5007. <https://doi.org/10.1109/TGRS.2016.2561938>.
- Chen, J., Li, J., Zhang, Z., Ni, S., 2014. Long-term groundwater variations in North-west India from satellite gravity measurements. *Glob. Planet. Change* 116, 130–138. <https://doi.org/10.1016/j.gloplacha.2014.02.007>.
- Cheng, M., Tapley, B.D., 2004. Variations in the earth's oblateness during the past 28 years. *J. Geophys. Res. Solid Earth* 109, B09402. <https://doi.org/10.1029/2004JB003028>.
- Colliander, A., Jackson, T.J., Bindlish, R., Chan, S., Das, N., Kim, S.B., Cosh, M.H., Dunbar, R.S., Dang, L., Pashaian, L., Asanuma, J., Aida, K., Berg, A., Rowlandson, T., Bosch, D., Caldwell, T., Caylor, K., Goodrich, D., Jassar, H., Lopez-Baeza, E., Martínez-Fernández, J., González-Zamora, A., Livingston, S., McNairn, H., Pacheco, A., Moghaddam, M., Montzka, C., Notarnicola, C., Niedrist, G., Pellarin, T., Prueger, J., Pulliainen, J., Rautiainen, K., Ramos, J., Seyfried, M., Starks, P., Su, Z., Zeng, Y., van der Velde, R., Thibeault, M., Dorigo, W., Vreugdenhil, M., Walker, J.P., Wu, X., Monerris, A., O'Neill, P.E., Entekhabi, D., Njoku, E.G., Yueh, S., 2017. Validation of SMAP surface soil moisture products with core validation sites. *Remote Sens. Environ.* 191, 215–231. <https://doi.org/10.1016/j.rse.2017.01.021>.
- Crow, W.T., Koster, R.D., Reichle, R.H., Sharif, H.O., 2005. Relevance of time-varying and time-invariant retrieval error sources on the utility of spaceborne soil moisture products. *Geophys. Res. Lett.* 32, L24405. <https://doi.org/10.1029/2005GL024889>.
- De Lannoy, G.J.M., Houser, P.R., Pauwels, V.R.N., Verhoest, N.E.C., 2006. Assessment of model uncertainty for soil moisture through ensemble verification. *J. Geophys. Res.* Atmos. 111, D10101. <https://doi.org/10.1029/2005JD006367>.
- De Lannoy, G.J.M., Reichle, R.H., 2016. Assimilation of SMOS brightness temperatures or soil moisture retrievals into a land surface model. *Hydrol. Earth Syst. Sci.* 20, 4895–4911. <https://doi.org/10.5194/hess-20-4895-2016>.
- Decker, M., 2015. Development and evaluation of a new soil moisture and runoff parameterization for the cable lsm including subgrid-scale processes. *J. Adv. Model. Earth Syst.* 7, 1788–1809. <https://doi.org/10.1002/2015MS000507>.
- Decker, M., Zeng, X., 2009. Impact of modified richards equation on global soil moisture simulation in the community land model (CLM3.5). *J. Adv. Model. Earth Syst.* 1 (5). <https://doi.org/10.3894/JAMES.2009.1.5>.
- Dong, J., Crow, W.T., Bindlish, R., 2017. The error structure of the SMAP single and dual channel soil moisture retrievals. *Geophys. Res. Lett.* 45, 758–765. <https://doi.org/10.1002/2017GL075656>.
- Dong, J., Crow, W.T., 2018. The added value of assimilating remotely sensed soil moisture for estimating summertime soil moisture - air temperature coupling strength. *Water Resour. Res.* 54, 6072–6084. <https://doi.org/10.1029/2018WR022619>.
- Dong, J., Steele-Dunne, S.C., Judge, J., van de Giesen, N., 2015. A particle batch smoother for soil moisture estimation using soil temperature observations. *Adv. Water Resour.* 83, 111–122. <https://doi.org/10.1016/j.advwatres.2015.05.017>.
- Dunne, S.C., Entekhabi, D., Njoku, E.G., 2007. Impact of multiresolution active and passive microwave measurements on soil moisture estimation using the ensemble Kalman smoother. *IEEE Trans. Geosci. Remote Sens.* 45, 1016–1028. <https://doi.org/10.1109/TGRS.2006.890561>.
- Eicker, A., Schumacher, M., Kusche, J., Döll, P., Schmed, H.M., 2014. Calibration/Data assimilation approach for integrating GRACE data into the watgap global hydrology model (WGHM) using an ensemble Kalman filter: first results. *Surv. Geophys.* 35, 1285–1309. <https://doi.org/10.1007/s10712-014-9309-8>.
- Entekhabi, D., Njoku, E.G., O'Neill, P.E., Kellogg, K.H., Crow, W.T., Edelstein, W.N., Entin, J.K., Goodman, S.D., Jackson, T.J., Johnson, J., Kimball, J., Piepmeier, J.R., Koster, R.D., Martin, N., McDonald, K.C., Moghaddam, M., Moran, S., Reichle, R., Shi, J.C., Spencer, M.W., Thurman, S.W., Tsang, L., Zyl, J.V., 2010. The soil moisture active passive (SMAP) mission. *Proc. IEEE* 98, 704–716. <https://doi.org/10.1109/JPROC.2010.2043918>.
- Entekhabi, D., Rodriguez-Iturbe, I., Castelli, F., 1996. Mutual interaction of soil moisture state and atmospheric processes. *J. Hydrol. Soil Moisture Obs.* 184, 3–17. [https://doi.org/10.1016/0022-1694\(95\)02965-6](https://doi.org/10.1016/0022-1694(95)02965-6).
- Flechtner, F., Morton, P., Watkins, M., Webb, F., 2014. Status of the GRACE follow-on mission. Gravity, Geoid and Height Systems. Springer, Cham, pp. 117–121, International Association of Geodesy Symposia. https://doi.org/10.1007/978-3-319-10837-7_15.
- Forman, B.A., Reichle, R.H., Rodell, M., 2012. Assimilation of terrestrial water storage from GRACE in a snow-dominated basin. *Water Resour. Res.* 48, W01507. <https://doi.org/10.1029/2011WR011239>.
- Giroto, M., De Lannoy, G.J.M., Reichle, R.H., Rodell, M., Draper, C., Bhanja, S.N., Mukherjee, A., 2017. Benefits and pitfalls of GRACE data assimilation: a case study of terrestrial water storage depletion in India. *Geophys. Res. Lett.* 44, 2017GL072994. <https://doi.org/10.1002/2017GL072994>.
- Houborg, R., Rodell, M., Li, B., Reichle, R., Zaitchik, B.F., 2012. Drought indicators based on model-assimilated gravity recovery and climate experiment (GRACE) terrestrial water storage observations. *Water Resour. Res.* 48, W07525. <https://doi.org/10.1029/2011WR011291>.
- Huffman, G.J., 1997. Estimates of root-mean-square random error for finite samples of estimated precipitation. *J. Appl. Meteorol.* 36, 1191–1201. [https://doi.org/10.1175/1520-0450\(1997\)036<1191:EORMSR>2.0.CO;2](https://doi.org/10.1175/1520-0450(1997)036<1191:EORMSR>2.0.CO;2).
- Huffman, G.J., Bolvin, D.T., Nelkin, E.J., Wolff, D.B., Adler, R.F., Gu, G., Hong, Y., Bowman, K.P., Stocker, E.F., 2007. The trmm multisatellite precipitation analysis (TMPA): Quasi-Global, multiyear, combined-sensor precipitation estimates at fine scales. *J. Hydrometeorol.* 8, 38–55. <https://doi.org/10.1175/JHM560.1>.
- Jasinski, M.F., Borak, J.S., Kumar, S.V., Mocko, D., Peters-Lidard, C.D., Rodell, M., Rui, H., Beaudoin, H.K., Vollmer, B.E., Arsenault, K.R., Li, B., Bolten, J.D., Tangdamrongsub, N., 2019. NCA-LDAS: Overview and analysis of hydrologic trends for the national climate assessment. *J. Hydrometeorol.* <https://doi.org/10.1175/JHM-D-17-0234.1>.
- Jekeli, C., 1981. Alternative Methods to Smooth the Earth's gravity Field (Scientific Report, 327). The Ohio State University, Columbus, OH, USA.
- Kerr, Y.H., Waldteufel, P., Richaume, P., Wigneron, J.P., Ferrazzoli, P., Mahmoodi, A., Bitar, A.A., Cabot, F., Gruhier, C., Juglea, S.E., Leroux, D., Mialon, A., Delwart, S., 2012. The SMOS soil moisture retrieval algorithm. *IEEE Trans. Geosci. Remote Sens.* 50, 1384–1403. <https://doi.org/10.1109/TGRS.2012.2184548>.
- Kim, E., 2017. Overview of SnowEx Year 1 Activities. Presented at the SnowEx Workshop, Longmont, CO, United States.
- Kolassa, J., Reichle, R.H., Liu, Q., Cosh, M., Bosch, D.D., Caldwell, T.G., Colliander, A., Collins, Holifield, Jackson, C., Livingston, T.J., Moghaddam, S.J., Starks, P.J., M., 2017. Data assimilation to extract soil moisture information from SMAP observations. *Remote Sens.* 9, 1179. <https://doi.org/10.3390/rs9111179>.
- Koster, R.D., Guo, Z., Yang, R., Dirmeyer, P.A., Mitchell, K., Puma, M.J., 2009. On the nature of soil moisture in land surface models. *J. Clim.* 22, 4322–4335. <https://doi.org/10.1175/2009JCLI2832.1>.
- Kowalczyk, E.A., Wang, Y.P., Law, R.M., Davies, H.L., McGregor, J.L., Abramowitz, G.S., 2006. The CSIRO Atmosphere Biosphere Land Exchange (CABLE) Model for Use in Climate Models and as an Offline Model. CSIRO Marine and Atmospheric Research Spendale, Vic. <https://doi.org/10.4225/08/5861556a9a51d>.
- Kumar, S.V., Jasinski, M., Mocko, D., Rodell, M., Borak, J., Li, B., Kato Beaudoin, H., Peters-Lidard, C.D., 2018. NCA-LDAS land analysis: development and performance of a multisensor, multivariate land data assimilation system for the national climate assessment. *J. Hydrometeorol.* <https://doi.org/10.1175/JHM-D-17-0125.1>, in pressed.
- Kumar, S.V., Reichle, R.H., Koster, R.D., Crow, W.T., Peters-Lidard, C.D., 2009. Role of subsurface physics in the assimilation of surface soil moisture observations. *J. Hydrometeorol.* 10, 1534–1547. <https://doi.org/10.1175/2009JHM1134.1>.
- Kumar, S.V., Zaitchik, B.F., Peters-Lidard, C.D., Rodell, M., Reichle, R., Li, B., Jasinski, M., Mocko, D., Getirana, A., De Lannoy, G., Cosh, M.H., Hain, C.R., Anderson, M., Arsenault, K.R., Xia, Y., Ek, M., 2016. Assimilation of gridded GRACE terrestrial water storage estimates in the North American land data assimilation system. *J. Hydrometeorol.* 17, 1951–1972. <https://doi.org/10.1175/JHM-D-15-0157.1>.
- Li, B., Rodell, M., Zaitchik, B.F., Reichle, R.H., Koster, R.D., van Dam, T.M., 2012. Assimilation of GRACE terrestrial water storage into a land surface model: Evaluation and potential value for drought monitoring in western and central Europe. *J. Hydrol.* 446–447, 103–115. <https://doi.org/10.1016/j.jhydrol.2012.04.035>.
- Lievens, H., Reichle, R.H., Liu, Q., De Lannoy, G.J.M., Dunbar, R.S., Kim, S.B., Das, N.N., Cosh, M., Walker, J.P., Wagner, W., 2017. Joint sentinel-1 and SMAP data assimilation to improve soil moisture estimates. *Geophys. Res. Lett.* 44, 2017GL073904. <https://doi.org/10.1002/2017GL073904>.
- Lievens, H., Tomer, S.K., Al Bitar, A., De Lannoy, G.J.M., Drusch, M., Dumedah, G., Hendricks Franssen, H.-J., Kerr, Y.H., Martens, B., Pan, M., Roundy, J.K., Vereecken, H., Walker, J.P., Wood, E.F., Verhoest, N.E.C., Pauwels, V.R.N., 2015. SMOS soil moisture assimilation for improved hydrologic simulation in

- the Murray Darling Basin, Australia. *Remote Sens. Environ.* 168, 146–162. <https://doi.org/10.1016/j.rse.2015.06.025>.
- Liu, P.W., Judge, J., Roo, R.D.D., England, A.W., Bongiovanni, T., 2016. Uncertainty in soil moisture retrievals using the SMAP combined active-passive algorithm for growing sweet corn. *IEEE J. Sel. Top. Appl. Earth Obs. Remote Sens.* 9, 3326–3339. <https://doi.org/10.1109/JSTARS.2016.2562660>.
- Maurer, E.P., Rhoads, J.D., Dubayah, R.O., Lettenmaier, D.P., 2003. Evaluation of the snow-covered area data product from modis. *Hydrol. Process.* 17, 59–71. <https://doi.org/10.1002/hyp.1193>.
- Moradkhani, H., Hsu, K.-L., Gupta, H., Sorooshian, S., 2005. Uncertainty assessment of hydrologic model states and parameters: Sequential data assimilation using the particle filter. *Water Resour. Res.* 41, W05012. <https://doi.org/10.1029/2004WR003604>.
- Niu, G.-Y., Yang, Z.-L., Dickinson, R.E., Gulden, L.E., Su, H., 2007. Development of a simple groundwater model for use in climate models and evaluation with gravity recovery and climate experiment data. *J. Geophys. Res. Atmos.* 112, D07103. <https://doi.org/10.1029/2006JD007522>.
- Pitman, A.J., 2003. The evolution of, and revolution in, land surface schemes designed for climate models. *Int. J. Climatol.* 23, 479–510. <https://doi.org/10.1002/joc.893>.
- Reager, J.T., Thomas, A.C., Sproles, E.A., Rodell, M., Beaudoin, H.K., Li, B., Famiglietti, J.S., 2015. Assimilation of GRACE terrestrial water storage observations into a land surface model for the assessment of regional flood potential. *Remote Sens.* 7, 14663–14679. <https://doi.org/10.3390/rs71114663>.
- Reichle, R.H., 2008. Data assimilation methods in the earth sciences. *Adv. Water Resour. Hydrol. Remote Sens.* 31, 1411–1418. <https://doi.org/10.1016/j.advwatres.2008.01.001>.
- Reichle, R.H., Crow, W.T., Koster, R.D., Sharif, H.O., Mahanama, S.P.P., 2008. Contribution of soil moisture retrievals to land data assimilation products. *Geophys. Res. Lett.* 35, L01404. <https://doi.org/10.1029/2007GL031986>.
- Reichle, R.H., Koster, R.D., 2003. Assessing the impact of horizontal error correlations in background fields on soil moisture estimation. *J. Hydrometeorol.* 4, 1229–1242. [https://doi.org/10.1175/1525-7541\(2003\)004<1229:ATIOHE>2.0.CO;2](https://doi.org/10.1175/1525-7541(2003)004<1229:ATIOHE>2.0.CO;2).
- Reichle, R.H., Koster, R.D., 2004. Bias reduction in short records of satellite soil moisture. *Geophys. Res. Lett.* 31, L19501. <https://doi.org/10.1029/2004GL020938>.
- Renzullo, L.J., van Dijk, A.I.J.M., Perraud, J.-M., Collins, D., Henderson, B., Jin, H., Smith, A.B., McJannet, D.L., 2014. Continental satellite soil moisture data assimilation improves root-zone moisture analysis for water resources assessment. *J. Hydrol.* 519, 2747–2762. <https://doi.org/10.1016/j.jhydrol.2014.08.008>.
- Ridler, M.-E., Madsen, H., Stisen, S., Bircher, S., Fensholt, R., 2014. Assimilation of SMOS-derived soil moisture in a fully integrated hydrological and soil-vegetation-atmosphere transfer model in Western Denmark. *Water Resour. Res.* 50, 8962–8981. <https://doi.org/10.1002/2014WR015392>.
- Rodell, M., Chen, J., Kato, H., Famiglietti, J.S., Nigro, J., Wilson, C.R., 2007. Estimating groundwater storage changes in the Mississippi River Basin (USA) using GRACE. *Hydrogeol. J.* 15, 159–166. <https://doi.org/10.1007/s10040-006-0103-7>.
- Rodell, M., Houser, P.R., Jambor, U., Gottschalk, J., Mitchell, K., Meng, C.-J., Arsenault, K., Cosgrove, B., Radakovich, J., Bosilovich, M., Entin, J.K., Walker, J.P., Lohmann, D., Toll, D., 2004. The global land data assimilation system. *Bull. Am. Meteorol. Soc.* 85, 381–394. <https://doi.org/10.1175/BAMS-85-3-381>.
- Rüdiger, C., Hancock, G., Hemakumara, H.M., Jacobs, B., Kalma, J.D., Martinez, C., Thyer, M., Walker, J.P., Wells, T., Willgoose, G.R., 2007. Goulburn river experimental catchment data set. *Water Resour. Res.* 43, W10403. <https://doi.org/10.1029/2006WR005837>.
- Senanayake, I.P., Yeo, I.-Y., Tangdamrongsub, N., Willgoose, G.R., Hancock, G.R., Wells, T., Fang, B., Lakshmi, V., Walker, J.P., 2019. An in-situ data based model to downscale radiometric satellite soil moisture products in the upper Hunter region of NSW, Australia. *J. Hydrol.* 572, 820–838. <https://doi.org/10.1016/j.jhydrol.2019.03.014>.
- Schumann, G., Lunt, D.J., Valdes, P.J., de Jeu, R.A.M., Scipal, K., Bates, P.D., 2009. Assessment of soil moisture fields from imperfect climate models with uncertain satellite observations. *Hydrol. Earth Syst. Sci.* 13, 1545–1553. <https://doi.org/10.5194/hess-13-1545-2009>.
- Su, H., Yang, Z.-L., Dickinson, R.E., Wilson, C.R., Niu, G.-Y., 2010. Multisensor snow data assimilation at the continental scale: the value of gravity recovery and climate experiment terrestrial water storage information. *J. Geophys. Res. Atmos.* 115, D10104. <https://doi.org/10.1029/2009JD013035>.
- Swenson, S., Chambers, D., Wahr, J., 2008. Estimating geocenter variations from a combination of GRACE and ocean model output. *J. Geophys. Res. Solid Earth* 113, B08410. <https://doi.org/10.1029/2007JB005338>.
- Swenson, S., Wahr, J., 2006. Post-processing removal of correlated errors in GRACE data. *Geophys. Res. Lett.* 33, L08402. <https://doi.org/10.1029/2005GL025285>.
- Tangdamrongsub, N., Han, S.-C., Decker, M., Yeo, I.-Y., Kim, H., 2018a. On the use of the GRACE normal equation of inter-satellite tracking data for estimation of soil moisture and groundwater in Australia. *Hydrol. Earth Syst. Sci.* 22, 1811–1829. <https://doi.org/10.5194/hess-22-1811-2018>.
- Tangdamrongsub, N., Han, S.-C., Tian, S., Schmied, H.M., Sutanudjaja, E.H., Ran, J., Feng, W., 2018b. Evaluation of groundwater storage variations estimated from GRACE data assimilation and state-of-the-art land surface models in Australia and the North China plain. *Remote Sens.* 10, 483. <https://doi.org/10.3390/rs10030483>.
- Tangdamrongsub, N., Han, S.-C., Yeo, I.-Y., 2017a. Enhancement of water storage estimates using GRACE data assimilation with particle filter framework. In: Presented at the 22nd International Congress on Modelling and Simulation (MODSIM). Hobart, Tasmania, Australia, pp. 1041–1047.
- Tangdamrongsub, N., Steele-Dunne, S.C., Gunter, B.C., Ditmar, P.G., Sutanudjaja, E.H., Sun, Y., Xia, T., Wang, Z., 2017b. Improving estimates of water resources in a semi-arid region by assimilating GRACE data into the PCR-GLOBWB hydrological model. *Hydrol. Earth Syst. Sci.* 21, 2053–2074. <https://doi.org/10.5194/hess-21-2053-2017>.
- Tangdamrongsub, N., Steele-Dunne, S.C., Gunter, B.C., Ditmar, P.G., Weerts, A.H., 2015. Data assimilation of GRACE terrestrial water storage estimates into a regional hydrological model of the Rhine River Basin. *Hydrol. Earth Syst. Sci.* 19, 2079–2100. <https://doi.org/10.5194/hess-19-2079-2015>.
- Tapley, B.D., Bettadpur, S., Ries, J.C., Thompson, P.F., Watkins, M.M., 2004. GRACE measurements of mass variability in the earth system. *Science* 305, 503–505. <https://doi.org/10.1126/science.1099192>.
- Tian, S., Tregoning, P., Renzullo, L.J., van Dijk, A.I.J.M., Walker, J.P., Pauwels, V.R.N., Allgeyer, S., 2017. Improved water balance component estimates through joint assimilation of GRACE water storage and SMOS soil moisture retrievals. *Water Resour. Res.* 53, 1820–1840. <https://doi.org/10.1002/2016WR019641>.
- Ukkola, A.M., Pitman, A.J., Decker, M., De Kauwe, M.G., Abramowitz, G., Kala, J., Wang, Y.-P., 2016. Modelling evapotranspiration during precipitation deficits: identifying critical processes in a land surface model. *Hydrol. Earth Syst. Sci.* 20, 2403–2419. <https://doi.org/10.5194/hess-20-2403-2016>.
- Vergnes, J.-P., Decharme, B., Alkama, R., Martin, E., Habets, F., Douville, H., 2012. A simple groundwater scheme for hydrological and climate applications: Description and offline evaluation over France. *J. Hydrometeorol.* 13, 1149–1171. <https://doi.org/10.1175/JHM-D-11-0149.1>.
- Wahr, J., Molenaar, M., Bryan, F., 1998. Time variability of the earth's gravity field: Hydrological and oceanic effects and their possible detection using GRACE. *J. Geophys. Res. Solid Earth* 103, 30205–30229. <https://doi.org/10.1029/98JB02844>.
- Weerts, A.H., El Serafy, G.Y.H., 2006. Particle filtering and ensemble Kalman filtering for state updating with hydrological conceptual rainfall-runoff models. *Water Resour. Res.* 42, W09403. <https://doi.org/10.1029/2005WR004093>.
- Wood, E.F., Roundy, J.K., Troy, T.J., van Beek, L.P.H., Bierkens, M.F.P., Blyth, E., de Roo, A., Döll, P., Ek, M., Famiglietti, J., Gochis, D., van de Giesen, N., Houser, P., Jaffé, P.R., Kollet, S., Lehner, B., Lettenmaier, D.P., Peters-Lidard, C., Sivapalan, M., Sheffield, J., Wade, A., Whitehead, P., 2011. Hyperresolution global land surface modeling: Meeting a grand challenge for monitoring earth's terrestrial water. *Water Resour. Res.* 47, W05301. <https://doi.org/10.1029/2010WR010090>.
- Wu, W., Geller, M.A., Dickinson, R.E., 2002. The response of soil moisture to long-term variability of precipitation. *J. Hydrometeorol.* 3, 604–613. [https://doi.org/10.1175/1525-7541\(2002\)003<0604:TROSMT>2.0.CO;2](https://doi.org/10.1175/1525-7541(2002)003<0604:TROSMT>2.0.CO;2).
- Xu, X., Tolson, B.A., Li, J., Staebler, R.M., Seglenieks, F., Haghnegahdar, A., Davison, B., 2015. Assimilation of SMOS soil moisture over the Great Lakes Basin. *Remote Sens. Environ.* 169, 163–175. <https://doi.org/10.1016/j.rse.2015.08.017>.
- Zaitchik, B.F., Rodell, M., Reichle, R.H., 2008. Assimilation of GRACE terrestrial water storage data into a land surface model: results for the Mississippi River Basin. *J. Hydrometeorol.* 9, 535–548. <https://doi.org/10.1175/2007JHM951.1>.